Journal of Macromolecular Science, Part A
Publication details, including instructions for authors and subscription information:
http://www.informaworld.com/smpp/title~content=t713597274

Bilayer Lipid Membrane-Semiconductor Junctions. Spectroscopic and Electrochemical Characterizations and Photoelectron Transfer

Janos H. Fendler[a]
[a] Department of Chemistry, Syracuse University, Syracuse, New York

To cite this Article Fendler, Janos H.(1990) 'Bilayer Lipid Membrane-Semiconductor Junctions. Spectroscopic and Electrochemical Characterizations and Photoelectron Transfer', Journal of Macromolecular Science, Part A, 27: 9, 1167 — 1185
To link to this Article: DOI: 10.1080/00222339009349684
URL: http://dx.doi.org/10.1080/00222339009349684

J. MACROMOL. SCI.—CHEM., A27(9–11), pp. 1167–1185 (1990)

BILAYER LIPID MEMBRANE-SEMICONDUCTOR JUNCTIONS. SPECTROSCOPIC AND ELECTROCHEMICAL CHARACTERIZATIONS AND PHOTOELECTRON TRANSFER

JANOS H. FENDLER

Department of Chemistry
Syracuse University
Syracuse, New York 13244-4100

ABSTRACT

Three different systems of glyceryl monooleate (GMO) bilayer lipid membrane (BLM) supported semiconductor particles have been prepared and characterized. A single composition of particulate semiconductor deposited on only one side of the BLM constituted System A, two different compositions of particulate semiconductors sequentially deposited on the same side of the BLM represented System B, and two different compositions of particulate semiconductors deposited on the opposite sides of the BLM made up System C. Effective refractive indices and optical thicknesses of GMO-BLM-supported In_2S_3 and ZnS particles (System A), determined by Brewster-angle and reflection measurements, allowed the assessment of the maximum sizes and the volume fractions of semiconductor particles to be on the order of 1200 Å and 0.3, respectively. Since semiconductor particles are highly porous structures, only the first layer of particulates penetrated into the BLM and were considered in the proposed equivalent circuit and band models. The presence of semiconductors on the BLM surface has been established by voltage-dependent capacitance measurements, absorption spectroscopy, and optical microscopy. Subsequent to the injection of H_2S,

the first observable change was the appearance of fairly uniform white dots on the black film. These dots rapidly moved around and grew in size, forming islands which then merged with themselves and with a second generation of dots, which ultimately led to a continuous film which continued to grow in thickness. Cyclic voltammetry established the current rectifying behavior for the semiconductor-particle-coated BLMs. CdS, ZnS, and In_2S_3 (System A) formed an n-type, while $Cu_{2-(x+y)}S$ (System A) behaved like a p-type, electrolyte-semiconductor (ES) junction. Semiconductor-semiconductor heterojunction (SS') formation was established for System C. Transfer of conduction-band electrons to dissolved oxygen (for the n-type ES junction) and across the membrane was considered to be responsible for the observed dark currents. Steady-state illumination of a CdS-containing BLM resulted in the prompt development of -150 to -200 mV (*cis* side negative) potential difference in an open circuit across the GMO BLM. This initial photovoltage, V_I, quickly decayed to a steady value, V_S (-100 to -150 mV). When the illumination was turned off, the potential difference across the GMO BLM decreased to its dark value in 3–4 minutes.

INTRODUCTION

Bilayer (black) lipid membranes (BLMs) are formed by brushing an organic solution of a surfactant (or lipid) across a pinhole (2–4 mm diameter) separating two aqueous phases [1–3]. Alternatively, BLMs can be formed from monolayers by the Montal-Mueller method [1]. In this method the surfactant, dissolved in an apolar solvent, is spread on the water surface to form a monolayer below the Teflon partitioning, which contains the pinhole (0.1–0.5 mm diameter). Careful injection of an appropriate electrolyte solution below the surface raises the water level above the pinhole and brings the monolayer into apposition to form the BLM. An advantage of the Montal-Mueller method is that it permits the formation of dissymmetrical BLMs. The initially formed film is rather thick and reflects white light with a gray color. Within a few minutes the film thins and the reflected light exhibits interference colors that ultimately turn black. At that point the film is considered to be bimolecular (40–60 Å thickness).

Separation of two aqueous solutions by the BLM allows electrical measurements by macroscopic electrodes. Precise capacitance, conduc-

tance, and impedance measurements, both in the absence and in the presence of ionophores, have contributed much to our understanding of impulse and ion-transport mechanisms [2]. Particularly significant has been the development of voltage clamping (i.e., holding the bilayer membrane at a predetermined potential and measuring the current flow) and single-channel recording [4–6].

Investigations of BLMs suffer from two major drawbacks. First, BLMs are notoriously unstable. Very rarely do they survive longer than a couple of hours. Second, voltage clamping provides information only on the transition from an open ion channel state to a closed ion channel state and not to events of the closed states. Current research in our laboratories is directed toward overcoming these disadvantages by stabilizing BLMs via polymerization or polymer coating and by developing simultaneous *in-situ* spectroscopic and electrical techniques [7–14] for monitoring functioning BLMs.

Concurrent with our developing simultaneous electrical and spectroscopic techniques, studies have been initiated for the incorporation of semiconductor particles into BLMs [7, 15]. Microcrystalline semiconductors have been fruitfully utilized in many photoconversion processes. Dispersed microcrystalline semiconductors offer a number of advantages. They have broad absorption spectra, high surface areas, and high extinction coefficients at appropriate band energies. They are relatively inexpensive and can be sensitized by doping, i.e., by chemical or physical modifications. Unfortunately, microcrystalline semiconductors also suffer from a number of disadvantages. Until recently they could not be reproducibly prepared as small (less than 20 nm in diameter), monodispersed particles. Small and uniform particles are needed to diminish nonproductive electron-hole recombinations. The smaller the semiconductor particles, the greater the chance of the escape of the charge carriers to the particle surface where the electron transfer can occur. There is a minimum size, however, which the particles must reach before absorption occurs at the bulk bandgap, i.e., before the polymolecular cluster becomes a semiconductor. The onset of semiconducting properties for CdS has been estimated to occur for particles whose diameters reach 6 nm.

It is difficult to maintain semiconductors in a dispersed state in solution for extended times in the absence of stabilizers. Stabilizers are bound to affect, of course, the photoelectrical behavior of semiconductors. Their modification and their coating by catalysts are, at present, more of an art than a science. Furthermore, the lifetime of electron-hole pairs in semiconductors is orders of magnitude shorter than the excited-state lifetime of typical organic sensitizers. This is due to the much faster electron-

hole recombinations in semiconductors than the diffusion-limited quenchings observed with organic sensitizers in homogeneous solutions. Quantum yields for charge separations in colloidal semiconductors are, therefore, disappointingly low. Some of these difficulties have been overcome by incorporating semiconductor particles into reversed micelles [16, 17], polymer films [18–22], surfactant vesicles [23–26], clays [27, 28], Vycor glass [29], and zeolites [30]. Studies have been initiated by using BLMs as matrices for colloidal particles.

EXPERIMENTAL SECTION

Glyceryl monooleate (GMO; Nucheck Preparation Company), $CdCl_2$, KCl, $NaNO_3$, $ZnCl_2$ (Baker Analyzed Reagents), $InCl_3$ (Alfa), $Pb(CH_3COO)_2$, $CuSO_4$ (Fisher Scientific), $AgNO_3$ (Matheson, Coleman and Bell), H_2S (Matheson Gas Products), and decane (+99% purity, Aldrich) were used as received. Water was purified using a Millipore Milli-Q system, provided with a 0.2-μm Millistack filter at the outlet.

RESULTS AND DISCUSSION

Three different systems have been investigated (Fig. 1). A single composition of particulate semiconductor deposited only on one side of the BLM constituted System A. Two different compositions of particulate semiconductors sequentially deposited on the same side of the BLM represent System B. Finally, two different compositions of particulate semiconductors deposited on the opposite sides of the BLM made up System C.

In the absence of additives or adventitious impurities, the BLM is an electrical insulator. Current flow, on the order of only 10^{-9}, was detected in the range of -0.10 to $+0.10$ V (Fig. 2a). The determined resistance and capacitance of a 1.00 mm diameter GMO BLM bathed in 0.10 *M* KCl, (3–5) $\times$ 10^8 ohm and 2.0–2.2 nF, agreed well with those reported previously (3×10^8 ohm, 0.380 μF/mm^2) [8, 31]. *In-situ* semiconductor formation on the BLM surface resulted in marked changes in the electrical response. Depending on the system, the current flow was found to increase asymmetrically and the BLM became very much more stable and longer lived. Electron transfer across biological membranes and their artificial analogs have been rationalized in terms of three different mechanisms [32]. The first model is the electronic conductance by direct elec-

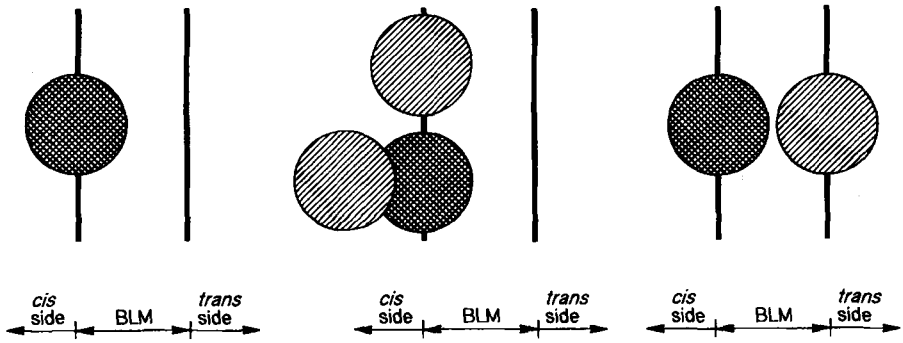

FIG. 1. Schematic representation of the different semiconductor-coated BLMs. A single composition of particulate semiconductor deposited only on one side of the BLM constitutes System A. Two different compositions of particulate semiconductors sequentially deposited on the same side of the BLM represents System B. Finally, two different compositions of particulates deposited on the opposite sides of the BLM make up System C.

tron tunneling. In the second model, electron transfer is considered to occur by electron hopping via impurity states. This is sometimes referred to as resonance tunneling. It is assumed in the third model that charge is carried by chemical species, i.e., the conductance is electrolytic.

Single-composition microcrystalline semiconductor particles incorporated onto only one side of the BLM represent the most straightforward system, already investigated in some detail by other methods [4–9]. The composition of the electrochemical cell used in investigating System A is explicitly shown in Eq. (1).

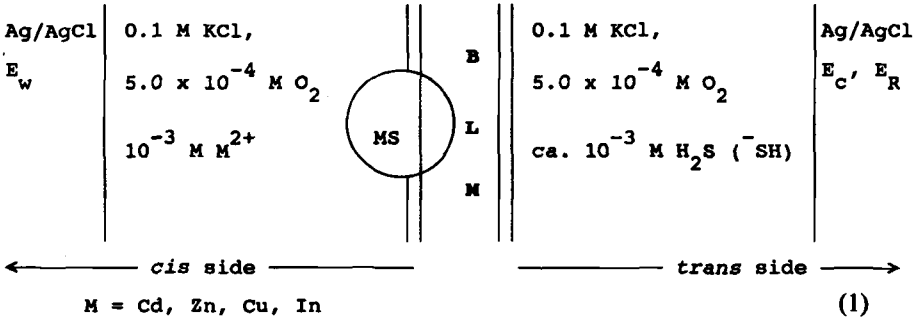

(1)

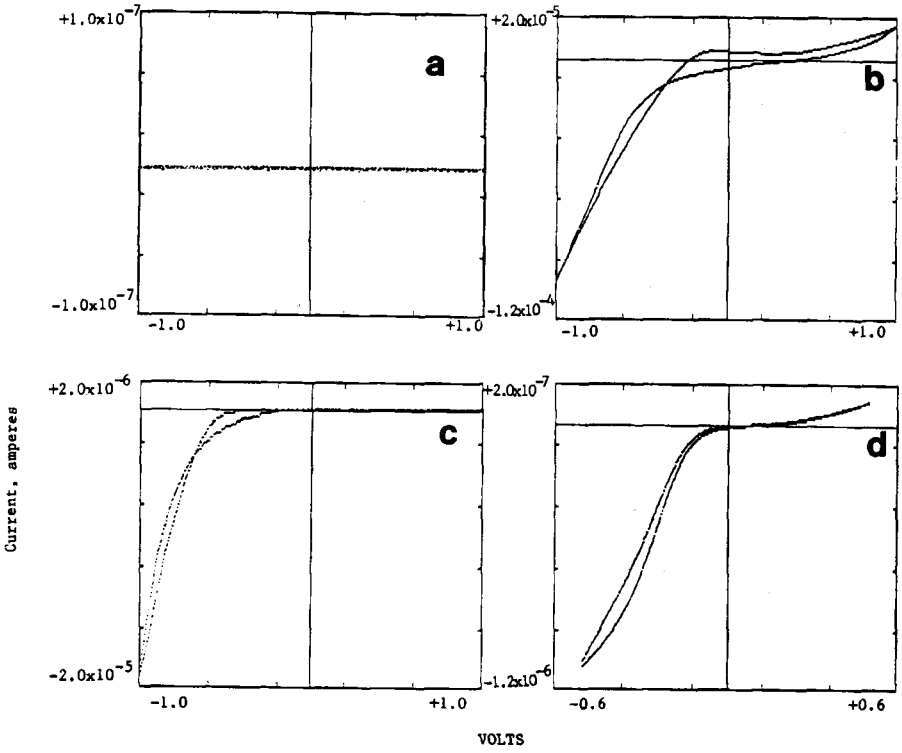

FIG. 2. Cyclic voltammograms of a GMO BLM in the absence (a) and in the presence of ZnS (b), CdS (c), and In_2S_3 (d) particles on its surface (System A). Scan rate: 100 mV/s.

where E_w, E_c, and E_R indicate the working, the counter, and the reference electrodes, respectively. Presumably, Systems B and C are also porous structures, explicitly shown in Eqs. (2) and (3) respectively.

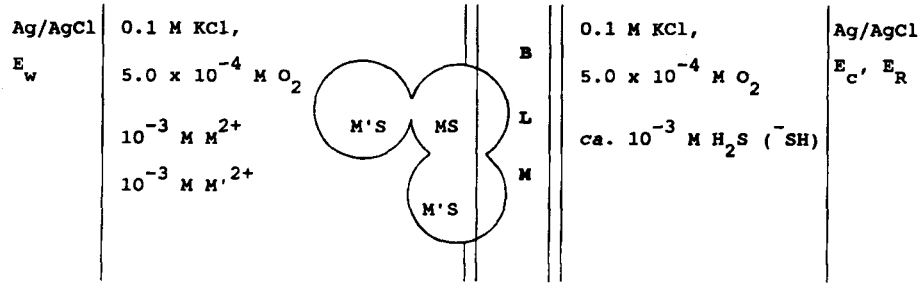

(2)

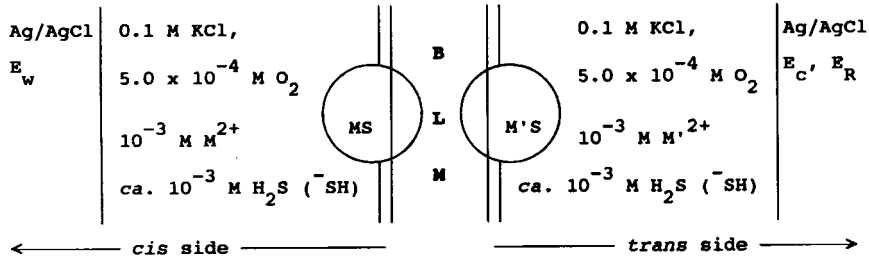

(3)

Equations (1), (2), and (3), as well as Fig. 1, are gross oversimplifications and should in no way be considered to convey any structural information beyond the location of the semiconductor particles and their penetration into the BLM.

Typical current-voltage, or I-V, curves of ZnS, CdS, In_2S_3, and $Cu_{2-(x+y)}S$ are illustrated in Figs. 2(b), 2(c), 2(d), and 3(b), respectively. The shapes and characteristics of the I-V curves remained essentially independent of the rate of scanning from 10 to 10^6 mV/s. Independence of cyclic voltammetric behavior on the frequency of scanning is used as a criterion to support electronic (as opposed to electrolytic) charge transfer mechanisms [33, 34]. Uncertainties in and nonlinearities of the resistances of BLM-incorporated semiconductor systems do not allow an unambiguous use of this criterion. Different semiconductor particles penetrate to different extents into the BLM. Although the membrane remained intact (as seen by the blackness of the reflected light), formation of microscopic defects cannot be excluded. Such pinholes would facilitate electrolytic charge transport. Similarly, the presence of adventitious and deliberately added (H_2S, O_2) dopants in the BLM matrix may well mediate resonance electron tunneling. Accordingly, electron transfer across a semiconductor-containing BLM may be governed either by electronic or by electrolytic conductance or indeed by some combination of both of these mechanisms. Regardless of the mechanism(s) involved, the role of the semiconductor particles is crucial. Different semiconductor particles have elicited substantially different current-voltage behavior (see Figs. 2 and 3) and the observed photovoltage action spectra corresponded to the absorption spectra of semiconductor particles deposited on the BLMs [8]. Pigmented [3] and protein- [34–37] containing BLMs behaved analogously. Their electrochemical responses also depended on the given pigment (or protein) incorporated into the BLM and on the potential of the redox species surrounding it.

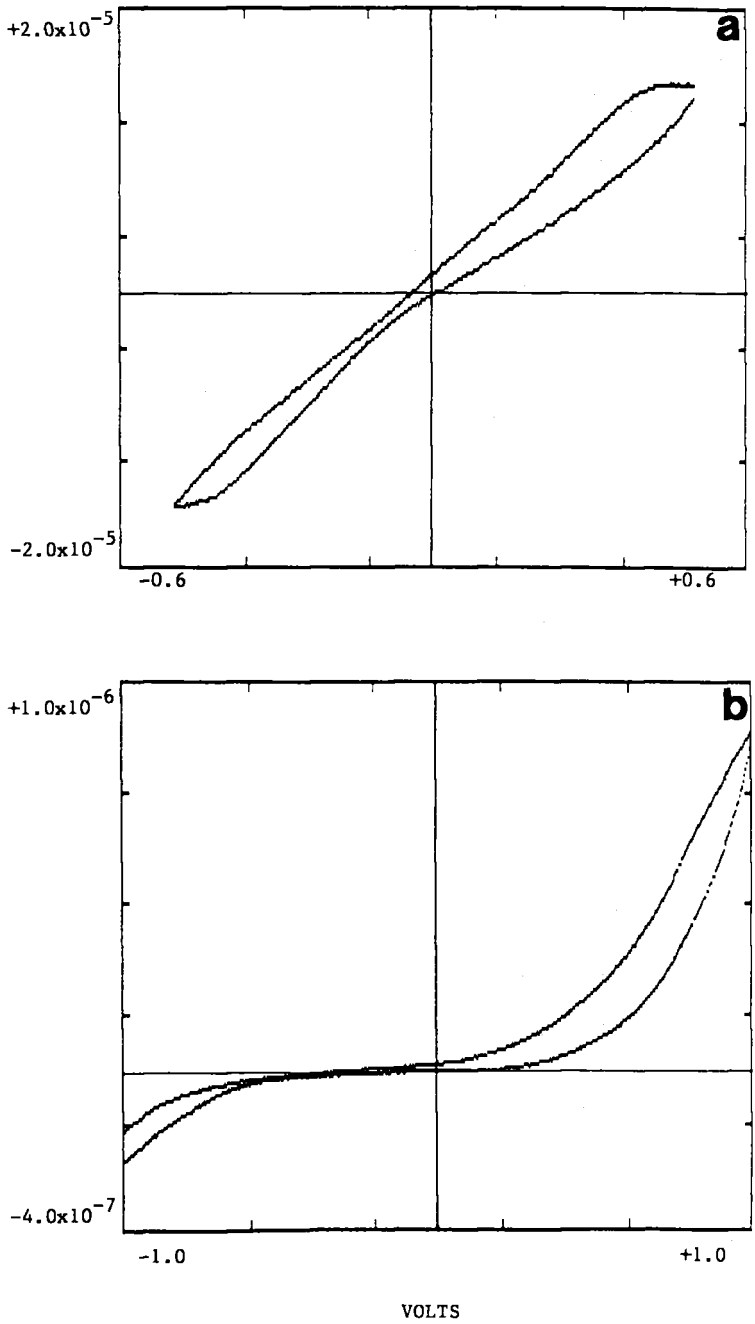

To a first approximation, the BLM can be considered to behave like a parallel plate capacitor immersed in a conducting electrolyte solution [3, 38].* The equivalent circuit describing the working (E_w), the reference (E_R), and the counter (E_c) electrodes; the resistance (R_m) and the capacitance (C_m) of the BLM; the resistance (R_H) and capacitance (C_H) of the Helmholtz electrical double layer surrounding the BLM; as well as the resistance of the electrolyte solution (R_{sol}) are shown in Fig. 4(a).

Deposition of a particulate semiconductor on the *cis* side of the BLM (System A) alters the equivalent circuit to that shown in Fig. 4(b) where R_f and C_f are the resistance and capacitance due to the particulate semiconductor film; R'_m and C'_m are the resistance and capacitance of the parts of the BLM which remained unaltered by the incorporation of the semiconductor particles; R_{sc} and C_{sc} are the space charge resistance and capacitance at the semiconductor particle–BLM interface; and R_{ss} and C_{ss} are the resistance and capacitance due to surface-state on the semiconductor particles in the BLM. Electrolytes short circuit the porous semiconductor particles ($R_f = R_{sol} = 1.4$ kΩ), and their contribution, along with that due to the Helmholtz layer, can be neglected. This allows the simplification of the equivalent circuit to that shown in Fig. 4(c). As seen, the working electrode is connected (via ions) to the semiconductor particulate film.

Band models [39, 40] of n- and p-type semiconductor-containing BLM- (System A) ES junctions are drawn in Fig. 5. Charge injection into the conduction band of the n-type semiconductor by a sufficiently active surface donor or by an applied voltage (making the *trans* side positive relative to the *cis* side) results in the accumulation of the majority carriers at the space-charge region (*cis*) surface of the semiconductor particles (Fig. 5a). The variation of potential with distance accompanying the

*There is no proof, of course, for making this assumption. In reality, even such a thin insulator as the modified BLM (designated by C'_m and R'_m in Fig. 4) could block the specific adsorption of some species from solution and/or modify the electrochemical behavior of the system. Similarly, System C may turn out to be an SIS′ rather than an SS′ junction. The present experiments, however, did not allow for an unambiguous distinction between these two alternative models, and we have chosen the simpler of the two.

FIG. 3. Cyclic voltammograms of the initial formation of semimetallic $Cu_{2-x}S$ (a) and its subsequent reduction to $Cu_{2-(x+y)}S$ (b) on the cis surface of a GMO BLM (System A). Scan rate: 100 mV/s from +1.0 to −1.0 V.

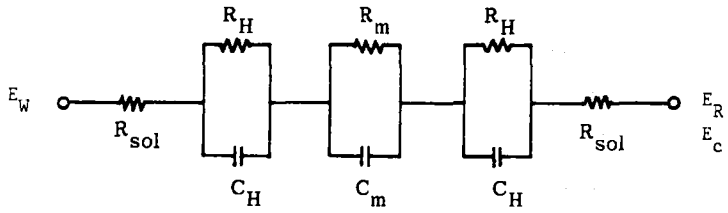

a

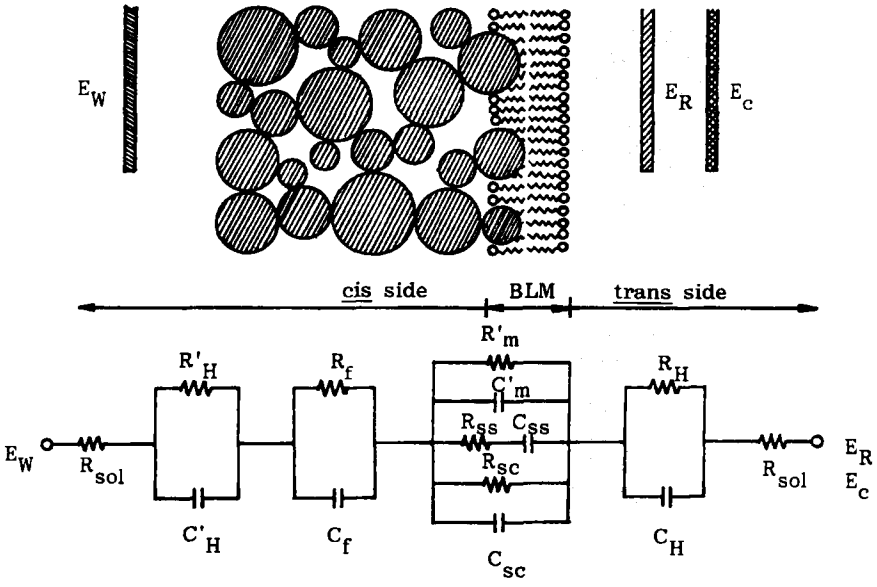

b

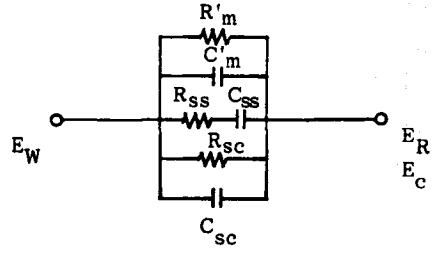

c

accumulation of the majority carrier in the space charge region (*cis* surface) is given by Poisson's relations as

$$\frac{d^2V}{dX_1^2} = \left(-\frac{{}^{n}\mathrm{B}^{e}}{\epsilon_s\epsilon_0}\right)[\exp\ (-eV/kT) - 1] \tag{4}$$

where $V(X_1) = \psi_b - \psi(X_1)$, ψ_b is the potential in the bulk of the semiconductor, n_B is the bulk density of the majority carrier, X_1 is the distance from the semiconductor *cis* surface (as shown in Fig. 5a), e is the electronic charge, ϵ_s is the dielectric constant of the semiconductor, k is Boltzmann's constant, T is the absolute temperature, and V is the applied potential. The first and second term in the right-hand side of Eq. (4) represent the contribution of electrons and immobile positive charges, respectively. Simple integration of Eq. (4) results in

$$\left(\frac{dV}{dX_1}\right)^2 = \left(\frac{2{}^{n}\mathrm{B}^{e}}{\epsilon_s\epsilon_0}\right)\left\{\left[\left(\frac{kT}{e}\right)\exp\left(\frac{-eV}{kT}\right) - 1\right] + V\right\} \tag{5}$$

Downward bending of the conduction-band energy (E_{cs}) provides for a favorable overlap with the energy level of the reducing agent (E_{red}) at the *cis* electrolyte surface, and the semiconductor particle provides an ohmic contact with the *cis* electrolyte. A depletion layer is formed at the particle surface which is immersed in the BLM, and Poisson's equation becomes

$$d^2V/dX_2^2 = {}^{e}N_{SC}/\epsilon_0\epsilon_s \tag{6}$$

FIG. 4. Proposed equivalent circuits for an "empty" (a) and a semiconductor-particle-coated (b) BLM. Porous structure of the semiconductor particles allowed the simplification of the equivalent circuit to that shown in (c). R_m, R_H, and R_{sol} are resistances due to the membrane, to the Helmholtz electrical double layer, and to the electrolyte solutions, respectively; while C_m and C_H are the corresponding capacitances; R_f and C_f are the resistance and capacitance due to the particulate semiconductor film; R'_m and C'_m are the resistance and capacitance of the parts of the BLM which remained unaltered by the incorporation of the semiconductor particles; R_{sc} and C_{sc} are the space charge resistance and capacitance at the semiconductor particle-BLM interface; and R_{ss} and C_{ss} are the resistance and capacitance due to surface-state on the semiconductor particles in the BLM.

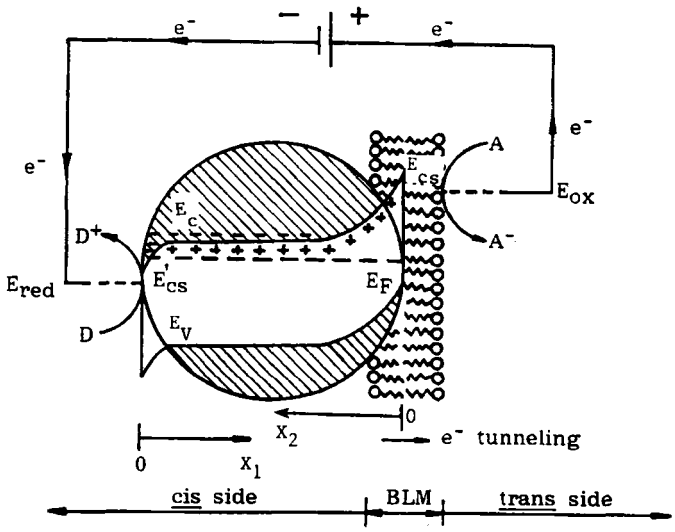

a

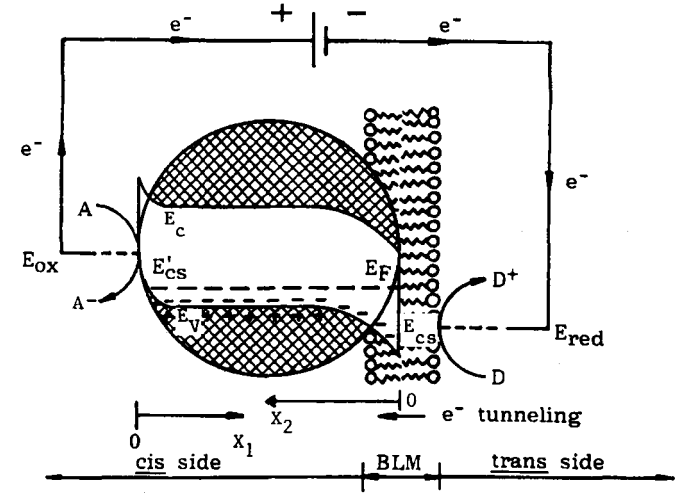

b

where N_{sc}, for an n-type semiconductor, is the density of the immobile positive charge in the space charge layer, and X_2 is the distance of the semiconductor–BLM interface (see Fig. 5a). Integrating twice, Eq. (6) results in

$$V = \frac{eN_{SC}}{2\epsilon_0\epsilon_s}(X_2 - W)^2 \tag{7}$$

where W is the depletion layer. At the surface $X_2 = 0$, the surface barrier, V_s, is given by

$$V_s = \frac{eN_{SC}W^2}{2\epsilon_0\epsilon_s} = \frac{E_{CS} - E_C}{e} \tag{8}$$

Hence, the conduction band energy, E_c, is upwardly bent to the energy of the conduction band edge at the surface, E_{cs}. Current flow is observed under cathodic (*trans* side positive with respect to the *cis* side) potential since E_{red} is located in the band-gap region. Electrons are assumed to tunnel through the modified, very thin BLM (or be transported by electrolytes) to the overlapping unoccupied energy levels of the oxidizing agent (E_{ox}). The exponential increase of cathodic current with applied voltage is the expected consequence of decreased band bending and increased surface electron densities. Behavior of the p-type semiconductor can be analogously rationalized.

Steady-state irradiation of a CdS-containing GMO BLM resulted in further decrease in resistance to about (0.5–3.0) $\times$ 10^8 ohms. The observed resistance drop was typically in the range of 20–25% with any particular CdS GMO BLM. Absence of a remarkable resistance change across the semiconductor-containing BLM upon steady-state irradiation is accountable in terms of incorporation of CdS into, rather than a fully spanned penetration across, the GMO BLM. When the light shutter was

FIG. 5. Band models for an n- (a) and a p- (b) type semiconductor-containing BLM- (System A) ES junction. E_{cs} and E'_{cs} represent the conduction-band edge at the semiconductor–BLM interface and at the semiconductor cis surface. E_F is the Fermi energy level, and E_{red} and E_{ox} are energy levels of the reducing and oxidizing agents, respectively. A and D stand for an electron acceptor and an electron donor, respectively.

opened, the potential difference across the BLM instantly reached a value between -150 and -200 mV, with the Ag/AgCl electrode on the *cis* side (the side of the BLM which contained the CdS particles) becoming negative. This initial photovoltage, defined as the change in the potential difference across the BLM caused by irradiation and designated as V_I, then quickly relaxed to a steady value, V_S. When the illumination was turned off, the observed potential difference across the BLM decayed to its dark value in approximately 3–4 minutes. Typical photovoltage signals from a CdS-containing GMO BLM are shown in Fig. 6.

Steady-state photocurrents were also determined at different bias voltages applied across the CdS-containing BLM. Advantage was taken of the ability of the patch clamp to hold a potential difference across the

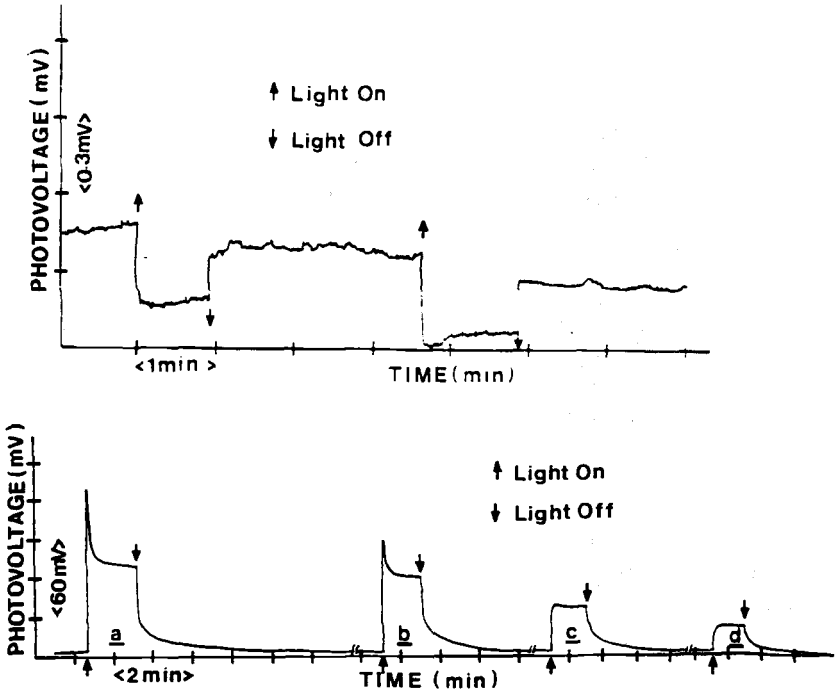

FIG. 6. Photovoltage signals obtained from a CdS-containing GMO BLM when illuminated with a steady-state lamp with 4.08×10^{-6} W (a), 0.89×10^{-6} W (b), 0.042×10^{-6} W (c), and 0.033×10^{-6} W (d) energies incident upon the GMO BLM. The upper plot indicates results of irradiation of the electrode (with the Teflon sleeve removed) in the absence of CdS.

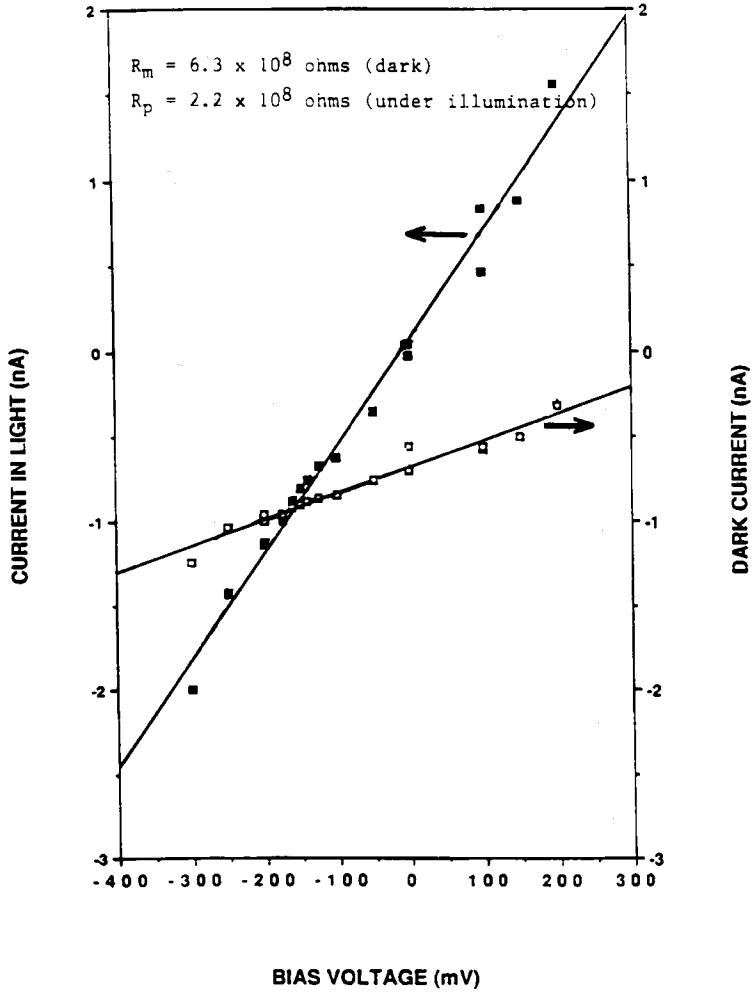

FIG. 7. Current passing through a CdS-containing GMO BLM as a function of the potential difference held across the BLM with a patch clamp in the dark (□) and in the present of light (4.0 × 10^{-6} W of energy incident upon the BLM; ■). The magnitude of the photocurrent at any voltage is given by the difference in the ordinate of the two points with the same abscissa (i.e., bias voltage).

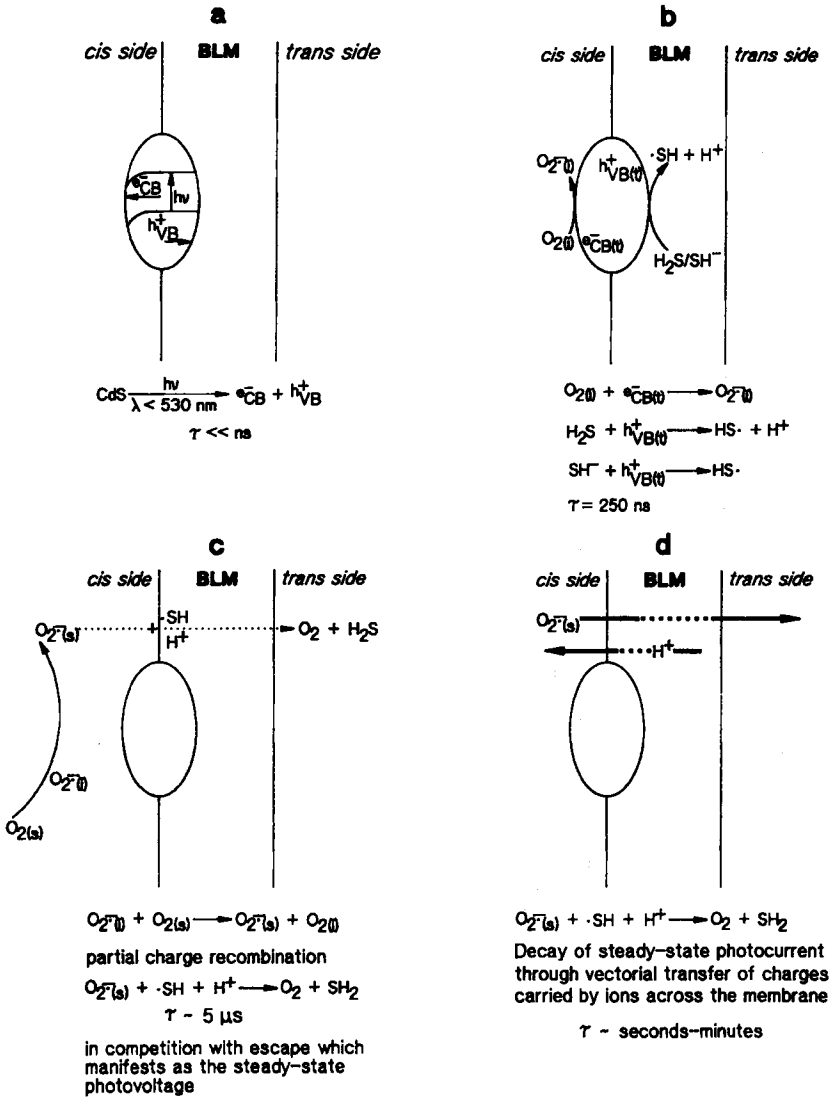

FIG. 8. Proposed chemical model for photovoltage generation across the CdS-containing GMO BLM. Reaction sites are highly speculative.

BLM at a predetermined value in the +400 and −400 mV range. Linear current–applied voltage behavior was observed for the CdS GMO BLM, both in the dark and under constant illumination (Fig. 7). The photocurrent at any particular voltage is given by the vertical difference between these two lines at that voltage. In the dark, the slope of the current–voltage curve was found to be small (1.6 pA/mV), corresponding to a composite resistance of the CdS-containing BLM (6.3×10^8 ohms).

The observed photoelectric effects are best accommodated in terms of light-induced vectorial transfer of charges across the BLM, carried by ions, in a direction opposite to the asymmetric BLM potential, ϕ_m (+426 mV). Absorption of light quanta with energy larger than 2.6 eV ($\lambda < 530$ nm), which is the bandgap of CdS, results in electron transfer from the valence to the conduction band of the semiconductor. Most of the free carriers undergo quick radiative and nonradiative recombinations at impurity or defect sites. A small number of the electrons ($e^-_{CB(t)}$) and holes ($h^+_{VB(t)}$), however, escape recombination by being trapped both in the bulk and at the surface of the BLM-supported polycrystalline CdS particles. The trapped electrons are transferred, in turn, to oxygen molecules absorbed at the semiconductor–water interfaces. Under the influence of the asymmetric potential, ϕ_m (+426 mV) in the CdS-containing GMO BLM, $e^-_{CB(t)}$ will move preferentially to the positive (*cis*) side and $h^+_{VB(t)}$ will migrate to the negative (*trans*) side of the membrane. The O_2^- radicals formed at the semiconductor interface are subsequently replaced by oxygen molecules present in the solution, $O_{2(s)}$, either by direct absorption–desorption processes or by electron transfer process. At the same time, hydrogen sulfide, H_2S, or its dissociated form, SH^- (which are permeable across the BLM and, hence, can approach both of its surfaces), are oxidized by the trapped holes.

Generation of O_2^- in the *cis* and H^+ in the *trans* side of the solution bathing the CdS-containing GMO BLM is the net chemical result of bandgap excitation. The observed photovoltage is then the consequence of vectorial transfer of charges, carried by ions, in a direction opposite to the asymmetric membrane potential. Figure 8 illustrates the proposed chemical model compatible with the equivalent circuit, illustrated in Fig. 4, for the generation of photovoltage across the CdS GMO BLM.

ACKNOWLEDGEMENT

Support of this research by a grant from the Department of Energy is gratefully acknowledged.

REFERENCES

[1] J. H. Fendler, *Membrane Mimetic Chemistry*, Wiley-Interscience, New York, 1982.

[2] H. T. Tien, *Bilayer Lipid Membranes (BLM). Theory and Practice*, Dekker, New York, 1974.

[3] P. Krysinski and H. T. Tien, *Prog. Surf. Sci., 23*, 317 (1986).

[4] C. Miller, *Ion Channel Reconstitution*, Plenum, New York, 1986.

[5] B. Hille, *Ionic Channels of Excitable Membranes*, Sinaver Associates, Sunderland, Massachusetts, 1984.

[6] B. Sakmann and E. Neher, *Single-Channel Recording*, Plenum, New York, 1983.

[7] S. Baral, X. K. Zhao, R. Rolandi, and J. H. Fendler, *J. Phys. Chem., 91* 2701 (1987).

[8] X. K. Zhao, S. Baral, R. Rolandi, and J. H. Fendler, *J. Am. Chem. Soc., 110*, 1012 (1988).

[9] S. Baral and J. H. Fendler, *Ibid., 111*, 1604 (1989).

[10] X. K. Zhao, P. J. Herve, and J. H. Fendler, *J. Phys. Chem., 93*, 908 (1989).

[11] X. K. Zhao and J. H. Fendler, *Ibid., 90*, 3886 (1986).

[12] R. Rolandi, S. R. Flom, I. Dillon, and J. H. Fendler, *Prog. Colloid Polym. Sci., 73*, 134 (1987).

[13] X. K. Zhao and J. H. Fendler, *J. Phys. Chem., 92*, 3350 (1988).

[14] X. K. Zhao, G. Picard, and J. H. Fendler, *Ibid., 92*, 7161 (1988).

[15] J. Kutnik and H. T. Tien, *Photochem. Photobiol., 46*, 413 (1987).

[16] M. Meyer, C. Wallberg, K. Kurihara, and J. H. Fendler, *J. Chem. Soc., Chem. Commun.*, p. 90 (1984).

[17] P. Lianos and J. K. Thomas, *Chem. Phys. Lett., 125*, 299 (1986).

[18] D. Meissner, R. Memming, and B. Kastening, *Ibid., 96*, 34 (1983).

[19] M. Krishnan, J. R. White, M. A. Fox, and A. J. Bard, *J. Am. Chem. Soc., 105*, 7002 (1983).

[20] A. W. H. Mau, C. B. Huang, N. Kakuta, A. J. Bard, A. Campion, M. A. Fox, M. J. White, and S. E. Webber, *Ibid., 106*, 6537 (1984).

[21] H. T. Tien, Z. C. Bi, and A. K. Tripathi, *Photochem. Photobiol., 44*, 779 (1986).

[22] J. P. Kuczynski, B. M. Milosavljevic, and J. K. Thomas, *J. Phys. Chem., 88*, 980 (1984).

[23] Y.-M. Tricot and J. H. Fendler, *J. Am. Chem. Soc., 106*, 2475 (1984).

[24] Y.-M. Tricot, A. Emeren, and J. H. Fendler, *Ibid., 89*, 4721 (1985).

[25] R. Rafaeloff, Y.-M. Tricot, F. Nome, P. Tundo, and J. H. Fendler, *J. Phys. Chem., 89*, 1236 (1985).

[26] H. C. Youn, Y.-M. Tricot, and J. H. Fendler, *Ibid., 91*, 581 (1987).
[27] O. Enea and A. J. Bard, *Ibid., 90*, 301 (1986).
[28] R. D. Stramel, T. Nakamura, and J. K. Thomas, *Chem. Phys. Lett., 130*, 43 (1986).
[29] J. Kuczynski and J. K. Thomas, *J. Phys. Chem., 89*, 2720 (1985).
[30] Y. Wang and N. Herron, *Ibid., 91*, 257 (1987).
[31] R. Fettiplace, *Biochim. Biophys. Acta, 513*, 1 (1978).
[32] S. U. M. Kahn, *J. Phys. Chem., 92*, 2541 (1988).
[33] A. J. Bard and L. R. Faulkner, *Electrochemical Methods*, Wiley, New York, 1980.
[34] M. A. Fox and M. Chanon (eds.), *Photoinduced Electron Transfer. Part A. Conceptual Basis*, Elsevier, Amsterdam, Holland, 1988. M. A. Habib and J. O'M. Bockris, *J. Bioelectr., 1*, 289 (1982).
[35] M. A. Habib and J. O'M. Bockris, *J. Bioelectr., 3*, 247 (1984).
[36] A. R. Michel, M. A. Habib, and J. O'M. Bockris, in *Electric Double Layer in Biology* (M. Blank, ed.), Plenum, New York, 1986, p. 167.
[37] M. A. Habib and J. O'M. Bockris, *J. Biophys., 14*, 31 (1986).
[38] F. T. Hong, *Photochem. Photobiol., 24*, 155 (1976).
[39] S. R. Morrison, *Electrochemistry at Semiconductor and Oxidized Metal Electrodes*, Plenum, New York, 1980.
[40] G. Hodes and M. Grätzel, *Nouv. J. Chim., 8*, 509 (1984).